Electronic Supplementary Material (ESI) for Materials Chemistry Frontiers.

Supporting Information

Fluorescence Visualization of Crystal Formation and Transformation Processes of Organic Luminogen with Crystallization-Induced Emission Characteristics

Chao Zheng, ‡[a] *Qiguang Zang,* ‡[a] *Han Nie,*[a] *Weitao Huang,*[a] *Zujin Zhao,*[a] *Anjun Qin,*[a] *Rongrong Hu,*[*, a] *and Ben Zhong Tang*[*, a, b]

[a] State Key Laboratory of Luminescent Materials and Devices, Center for Aggregation-Induced Emission, South China University of Technology, Guangzhou 510640, China.

[b] Department of Chemistry, The Hong Kong University of Science & Technology, Clear Water Bay, Kowloon, Hong Kong

‡ These authors contributed equally.

Table of Contents

Fig. S2 (A) Absorption spectrum of PPQE in THF solution. Concentration: 10 μM; (B) UV-Vis reflectance spectra of single crystals A–C.

Fig. S3 Time-resolved PL spectra of single crystals A (λ_{em} = 580 nm), B (λ_{em} = 590 nm), and C (λ_{em} = 562 nm). λ_{ex} = 470 nm.

Fig. S4 (A) PL spectra of PPQE in THF/water mixtures with different water contents (f_w). (B) Time-dependent PL spectra of PPQE in THF/water mixture with 99 vol% water content. Concentration: 10 μM; λ_{ex} = 424 nm.

Fig. S5 Calculated molecular orbital amplitude plots and energy levels of HOMOs and LUMOs for single crystals A–C.

Table S3. The representative Raman peaks and their corresponding motion modes of crystals A-C and the amorphous state of PPQE.

Fig. S6 Simulated XRD patterns from single crystal structures of (A) crystal A, (B) crystal B, and (C) crystal C; experimental XRD patterns of (D) needle-shaped crystal and (E) bulk crystal produced in the single crystal transformation process; experimental XRD patterns of fresh amorphous sample (F) before and (G) after 48 h at room temperature.

Fig. S7 Fluorescence microscopic images of single crystal A (A) before and (B) after been placed in saturated CH_3CN solution of PPQE for 2 days. Raman spectra of (C) single crystal A, (D and E) different domains of the crystal in (B), and (F) single crystal B.

Fig. S8 Raman spectra of the fresh amorphous PPQE (A) before and after (B) 48 h at room-temperature or (C) 0.5 h at 100 ^{o}C.

Fig. S9 DSC heating curve of amorphous PPQE.

Fig. S10 Fluorescence microscopic images of (A-E) time-dependent crystal growth process in acetone/*t*-butanol mixed solution of PPQE on a glass substrate. (F-J) Magnified fluorescence images of the time-dependent detailed transition states.

Fig. S11 Microscopic images of (A) sheet-like crystal line and (B) needle-shaped crystal line under daylight, (C) Raman spectra of these two different crystals.

Video S1. Fluorescence images of crystal formation process from amorphous solid.

Video S2. Fluorescence images of crystal formation process from solution.

Video S3. Magnified fluorescence images of crystal formation process from solution.

Synthesis of 1,4-diphenylbut-2-yne-1,4-dione (3)

Into a 100 mL two-necked round-bottom flask was added *trans*-1,2-dibenzoylethylene (**1**, 0.02 mol, 4.73 g) and 20 mL of chloroform. The reaction was stirred at 0 ℃, and liquid bromine (0.024 mol, 1.23 mL) was added slowly. The mixture was then stirred at room temperature for 5 hours and poured into a large amount of aqueous solution of sodium thiosulfate. The mixture was extracted by DCM. After removal of the solvents, the crude product **2** was obtained without further purification. The crude product **2**, trimethylamine (0.042 mol, 5.8 mL) and 50 mL of acetone were added into a 100 mL two-necked round-bottom flask. The mixture was stirred at 50 ℃ for 2 hours. After cooled to room temperature, the solvent was removed and the product was recrystallized in ethanol to obtain 3.42 g of yellow crystal **3** (yield = 73%).

Synthesis of PPQE

Into a 10 mL two-necked round-bottom flask was added **3** (0.001 mol, 0.23 g), *o*-phenylenediamine (0.001 mol, 0.11 g), and 3 mL of acetonitrile. The reaction mixture was refluxed at 95 ℃ for 5 hours, which was cooled to room temperature slowly to obtain orange crystals. The crystals were washed by acetonitrile to produce 0.28 g of pure PPQE crystals (yield = 85%). ^{1}H NMR ($CDCl_3$, 500 MHz): δ (ppm) 15.84 (s, 1H), 7.93 (d, J = 8.0 Hz, 1H), 7.85-7.68 (m, 4H), 7.65-7.50 (m, 5H), 7.48-7.36 (m, 4H), 6.40 (s, 1H). ^{13}C NMR ($CDCl_3$, 125 MHz): δ (ppm) 181.51, 156.81, 147.63, 138.14, 137.23, 137.11, 132.16, 130.93, 130.81, 129.82, 129.25, 128.85, 128.76, 128.49, 126.58, 126.02, 119.62, 91.21. HRMS: *m*/*z* 325.1333 ($M + H^+$, calcd 325.1335).

Preparation of polymorphs and amorphous sample of PPQE.

Single crystal A was obtained either by direct slow crystallization from the concentrated acetonitrile reaction mixture which was cooling from 95 ^{o}C oil-bath with about 1 ^{o}C/min rate, or by recrystallization from a concentrated DMSO solution of PPQE. The single crystal structure of crystal A has been reported in literature.[1] Single crystal B was obtained by recrystallization from acetonitrile solution of PPQE with a moderate concentration of 12.5 mg/mL, which was cooling in oil-bath from 95 ^{o}C with about 1 ^{o}C/min rate. The single crystal structure of crystal B has been reported in literature.[2] Single crystal C was obtained through recrystallization from dilute acetonitrile solution of PPQE with a concentration of 6 mg/mL at 80 ^{o}C with fast cooling in air. The glass-like red amorphous sample of PPQE can only be obtained by fast cooling the molten PPQE in liquid nitrogen.

Single crystal transformation process.

100 mg PPQE was dissolved in 8 mL acetonitrile at 80 ^{o}C and the warm solution was quickly transferred to a culture dish with a diameter of 6 cm at room-temperature. The culture dish was sealed to prevent from solvent evaporation during the crystal formation and transformation processes. Needle-shaped crystal C was formed quickly after a few minutes, and then a time-dependent in-situ single crystal transformation from crystal C to crystal B was observed at room-temperature in the saturated acetonitrile solution.

Crystal formation from amorphous sample.

PPQE sample between two slides of glasses was melted and was then quickly placed into liquid nitrogen to give rise to as-prepared amorphous sample of PPQE. The time-dependent amorphous to crystal transition was directly observed through a fluorescence microscope.

Crystal formation from solution and scratch-induced crystal formation and assembly.

10.0 mg of PPQE was dissolved in a mixed solvent of 2.0 mL of acetone and 0.5 mL of tertiary butanol to form a solution. On a clean and smooth glass microslide, three drops of the solution was added. After 15 seconds, a steel needle was used to scratch the surface of the microslide through the area covered by the solution. The pinpoint of the needle is tilted to make sure there are two contact points between the needle and the glass. Two different crystal line of polymorphs can then be seen through microscope within one minute.

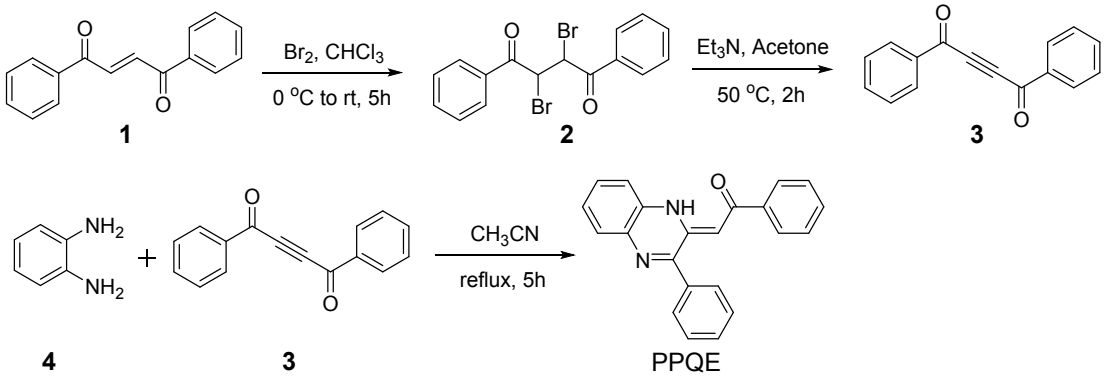

Scheme S1. Synthetic routes to PPQE.

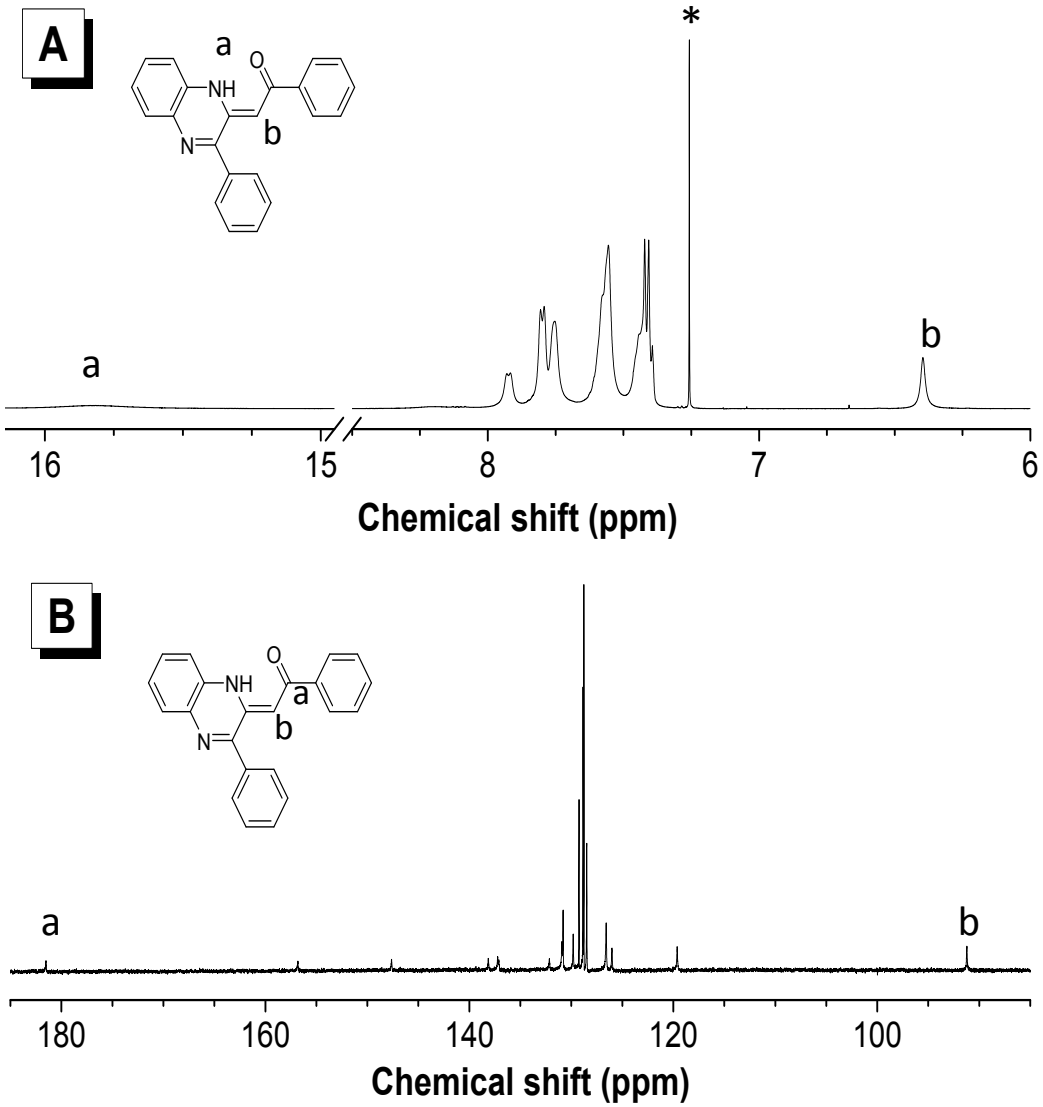

Fig. S1 (A) ^{1}H NMR and (B) ^{13}C NMR spectra of PPQE.

Table S1. Single crystal preparation in various solvents with different concentrations.

no.	[PPQE] (mg/mL)	solvents	polymorphs[a]
1	200	DMSO[b]	crystal A
2	40	CH_2Cl_2	crystal B
3	20	CH_2Cl_2/CH_3CN	crystal B
4	20	THF/CH_3CN	crystal B
5	16	CH_3CN[c]	crystal B
6	16	acetone[c]	crystal B
7	10	acetone/CH_3CN	crystal B
8	10	acetone/ petroleum ether	crystal B
9	10	acetone/CH_3OH	crystal B
10	20	THF/ petroleum ether	crystals B+C
11	20	CH_2Cl_2/CH_3OH	crystal C
12	20	CH_2Cl_2/ petroleum ether	crystal C
13	20	CH_2Cl_2/hexane	crystal C
14	10	THF/CH_3OH	crystal C
15	40	THF	crystal C
16	40	$CHCl_3$	crystal C

[a]Determined by the measurement of single crystal unit cell parameters; [b]Recrystallization via cooling the DMSO solution from 130 ^oC; [c]the sample was dissolved at 80 ^oC.

Table S2. Single crystal data for single crystals A–C.

Crystal form	crystal A	crystal B	crystal C
CCDC number	1500090	1500091	1500092
Empirical formula	$C_{22}H_{16}N_2O$	$C_{22}H_{16}N_2O$	$C_{22}H_{16}N_2O$
Formula weight	324.37	324.37	324.37
Temperature (K)	293 (2)	293 (2)	293 (2)
Wavelength (Å)	0.71073	0.71073	0.71073
Crystal system, space group	triclinic, P-1	triclinic, P-1	monoclinic, $P_{1\,21}/c_{\,1}$
Unit cell dimensions	a = 8.7512(9) Å b = 8.8377(10) Å c = 11.1832(10) Å α = 90.101(8)° β = 91.344(8)° γ = 106.984(9)°	a = 9.2692(8) Å b = 9.9355(10) Å c = 10.8222(9) Å α = 79.332(8)° β = 65.483(8)° γ = 69.001(9)°	a = 10.8856(12) Å b = 5.8214(6) Å c = 26.159(3) Å α = 90° β = 95.577(13)° γ = 90°
Volume (Å^3)	826.93 (15)	845.80(13)	1649.9(3)
Z, Calculated density (g cm^{-3})	2, 1.303	2, 1.274	4, 1.306
Absorption coefficient (mm^{-1})	0.081	0.079	0.081
F(000)	340	340	680
Crystal size, mm	0.38 × 0.26 × 0.24	0.38 × 0.32 × 0.23	0.48 × 0.23 × 0.2
Theta range for data collection	2.88 to 25.35°	3.84 to 25.35°	3.13 to 25.35°
Limiting indices	-10 <= h <= 10 -10 <= k <= 8 -13 <= l <= 13	-9 <= h <= 11 -9 <= k <= 11 -12 <= l <= 13	-13 <= h <= 10 -6 <= k <= 7 -31 <= l <= 31
Reflections collected / unique	5128 / 3021 [*R*(int) = 0.0457]	5305 / 3075 [*R*(int) = 0.0391]	6398 / 2992 [*R*(int) = 0.0508]
Completeness to theta	99.6%	99.6%	99.8%
Max. and min. transmission	1.00000 and 0.93821	1.00000 and 0.77304	1.00000 and 0.37556
Refinement method	Full-matrix least-squares on F^2		
Data / restraints / parameters	3021 / 0 / 226	3075 / 0 / 226	2992 / 0 / 226

Goodness-of-fit on F^2	1.027	1.033	1.035
Final R indices [$I > 2\text{sigma}(I)$]	R1 = 0.0485, wR2 = 0.1377	R1 = 0.0516, wR2 = 0.1220	R1 = 0.0576, wR2 = 0.1377
R indices (all data)	R1 = 0.1139, wR2 = 0.1439	R1 = 0.0808, wR2 = 0.1468	R1 = 0.0968, wR2 = 0.1653
Largest diff. peak and hole	0.158 and -0.213 e. Å^{-3}	0.230 and -0.227 e. Å^{-3}	0.196 and -0.192 e. Å^{-3}

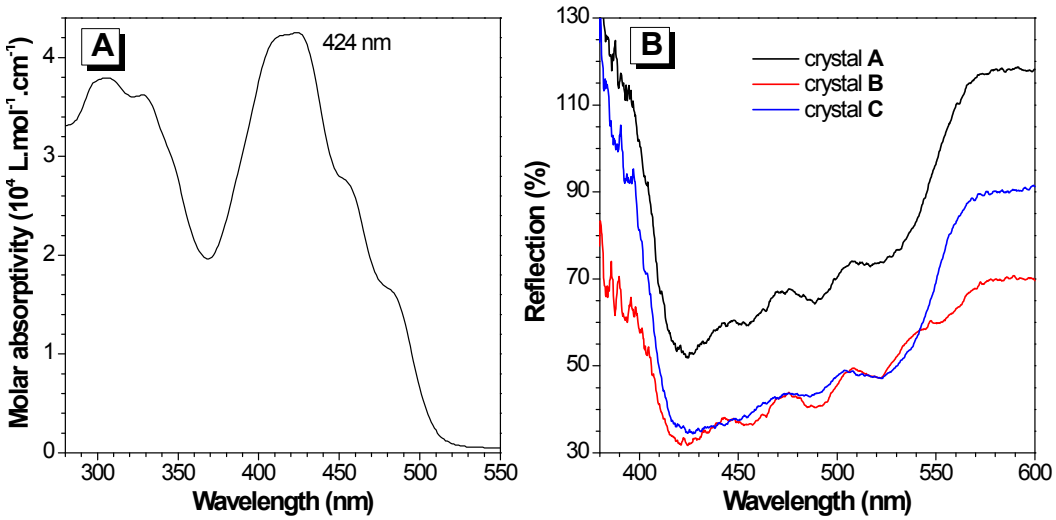

Fig. S2 (A) Absorption spectrum of PPQE in THF solution. Concentration: 10 μM; (B) UV-Vis reflectance spectra of single crystals A–C.

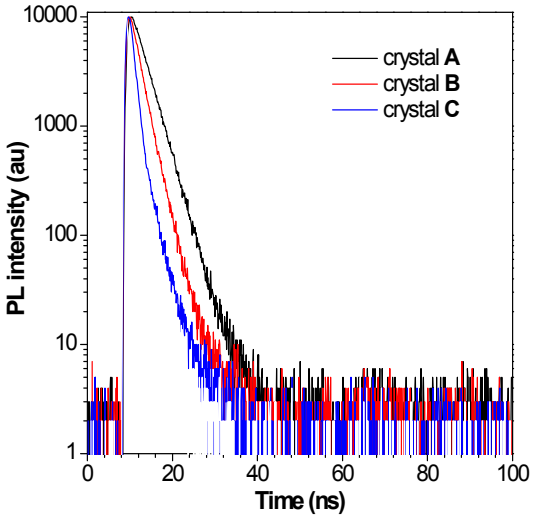

Fig. S3 Time-resolved PL spectra of single crystals A (λ_{em} = 580 nm), B (λ_{em} = 590 nm), and C (λ_{em} = 562 nm). λ_{ex} = 470 nm.

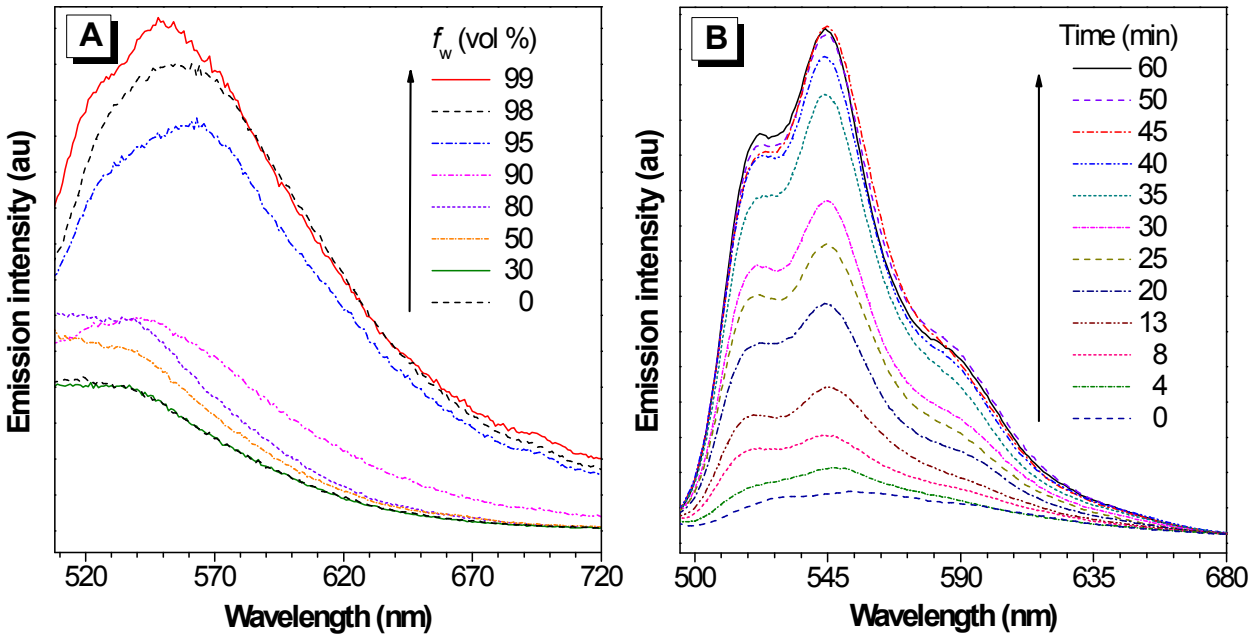

Fig. S4 (A) PL spectra of PPQE in THF/water mixtures with different water contents (f_w). (B) Time-dependent PL spectra of PPQE in THF/water mixture with 99 vol% water content. Concentration: 10 μM; λ_{ex} = 424 nm.

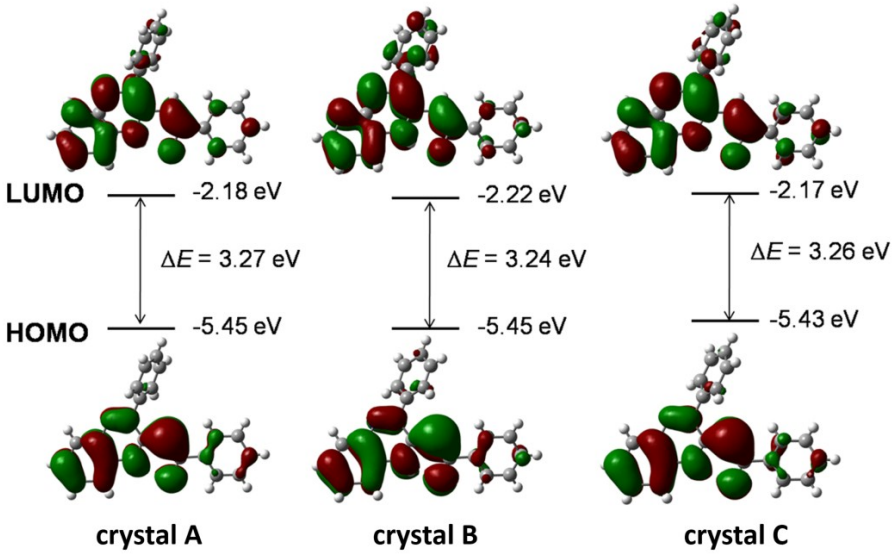

Fig. S5 Calculated molecular orbital amplitude plots and energy levels of HOMOs and LUMOs for single crystals A–C.

Table S3. The representative Raman peaks and their corresponding motion modes of crystals A-C and the amorphous state of PPQE.

peak	motion mode	crystal A	crystal B	crystal C	amor.
a	the swing between hydrogen atoms and the dihydroquinoxaline ring	1149	1146	1140	1148
b	the stretching vibration of the terminal phenyl ring	1172	1177	1172	1174
c	the twisting vibration betweem the terminal phenyl ring and the dihydroquinoxaline ring	1247	1247	1242	1247
d	the swing between hydrogen atoms and aromatic rings skeleton	1326	1329	1324	1329
e	the stretching vibration of the α-carbonyl ethylene group	1406	1398	1410	1407

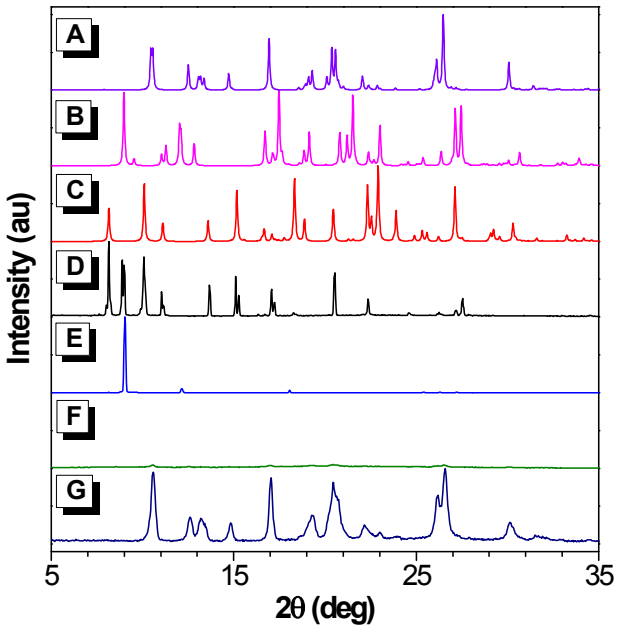

Fig. S6 Simulated XRD patterns from single crystal structures of (A) crystal A, (B) crystal B, and (C) crystal C; experimental XRD patterns of (D) needle-shaped crystal and (E) bulk crystal produced in the single crystal transformation process; experimental XRD patterns of fresh amorphous sample (F) before and (G) after 48 h at room temperature.

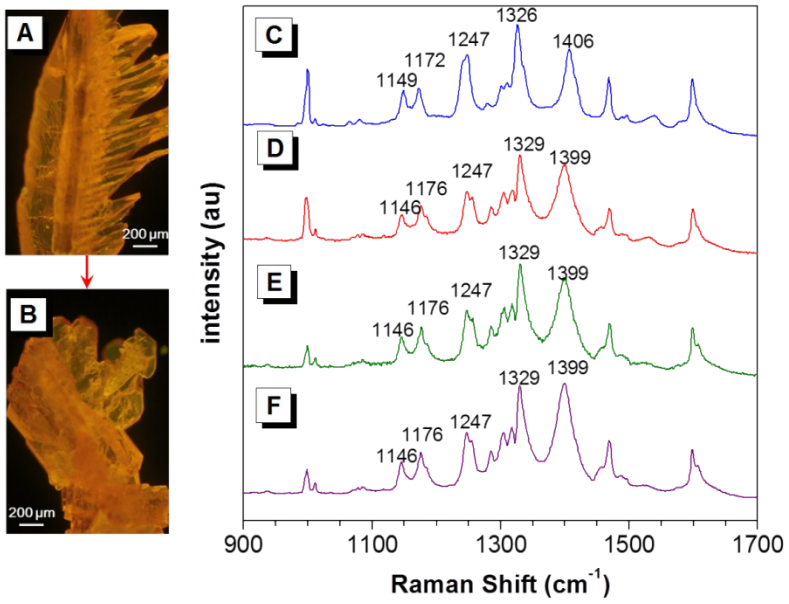

Fig. S7 Fluorescence microscopic images of single crystal A (A) before and (B) after been placed in saturated CH_3CN solution of PPQE for 2 days. Raman spectra of (C) single crystal A, (D and E) different domains of the crystal in (B), and (F) single crystal B.

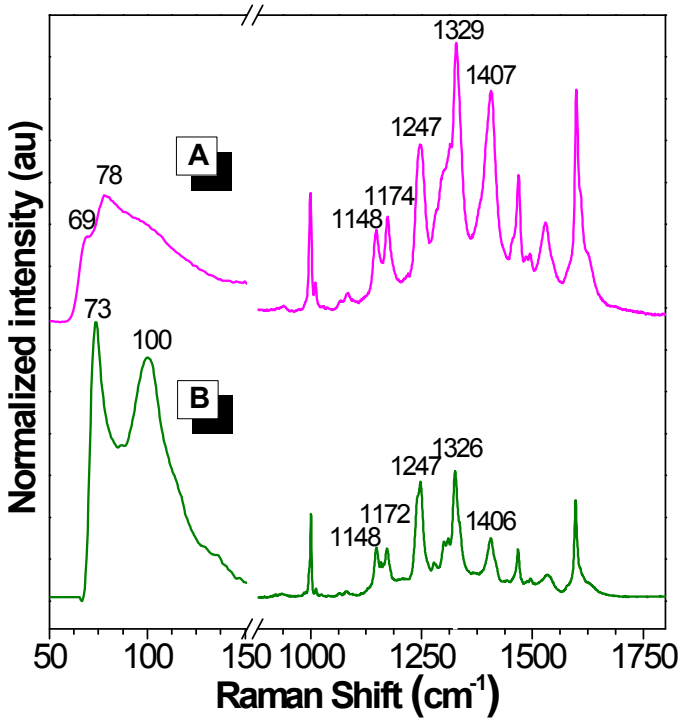

Fig. S8 Raman spectra of the fresh amorphous PPQE (A) before and after (B) 48 h at room-temperature.

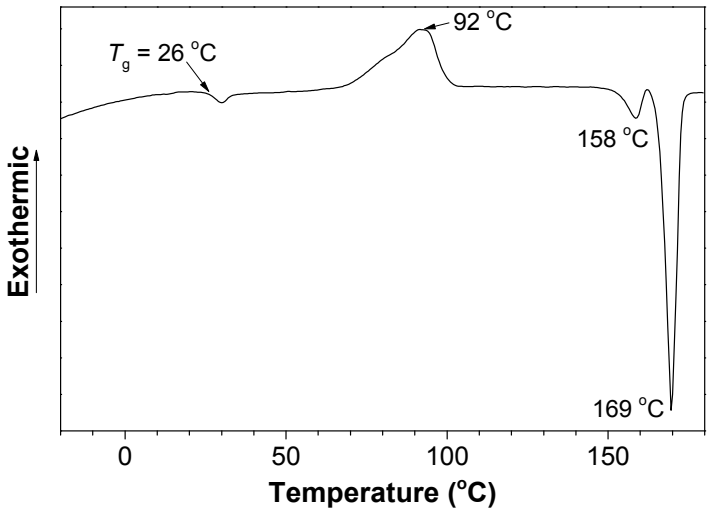

Fig. S9 DSC heating curve of amorphous PPQE.

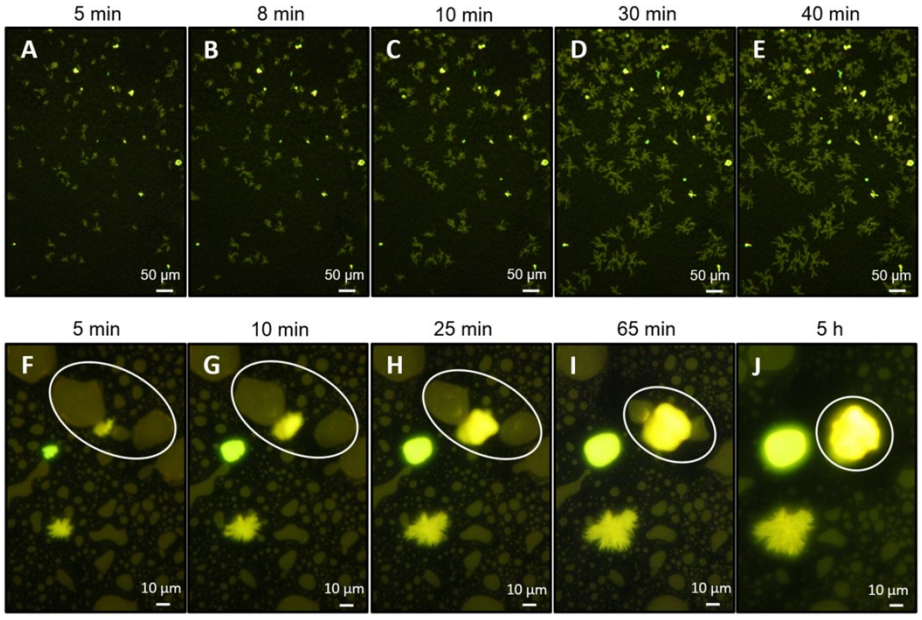

Fig. S10 Fluorescence microscopic images of (A-E) time-dependent crystal growth process in acetone/*t*-butanol mixed solution of PPQE on a glass substrate. (F-J) Magnified fluorescence images of the time-dependent detailed transition states.

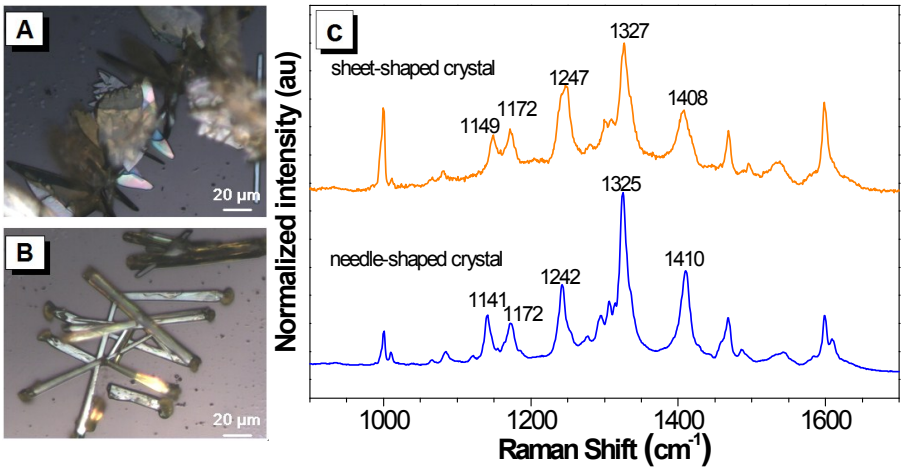

Fig. S11 Microscopic images of (A) sheet-like crystal line and (B) needle-shaped crystal line under daylight, (C) Raman spectra of these two different crystals.

Reference

1. D. Zhang, Y. Yang, M. Gao, W. Shu, L. Wu, Y. Zhu and A. Wu, *Tetrahedron*, 2013, **69**, 1849-1856.
2. M. I. Ansari, R. Shankar, M. K. Hussain, R. Kant, P. R. Maulik, K. R. Kumar and K. Hajela, *J. Heterocyclic Chem.* 2011, **48**, 1336-1341.